Applied Physics Express

LETTER

Finite differential hot-wire method for localized heat transfer characterization at microscale

Applied Physics Express 13, 105003 (2020)
https://doi.org/10.35848/1882-0786/abb870

LETTER

Finite differential hot-wire method for localized heat transfer characterization at microscale

Jianshu Gao[1], Danmei Xie[1*], Kai Cai[1], Yu Chen[1], and Yanan Yue[1,2*]

[1]School of Power and Mechanical Engineering, Wuhan University, Wuhan, Hubei 430072, People's Republic of China
[2]Department of Mechanical and Manufacturing Engineering, Miami University, Oxford, Ohio 45056, United States of America

*E-mail: dmxie@whu.edu.cn; yyue@whu.edu.cn

Received July 12, 2020; revised August 31, 2020; accepted September 13, 2020; published online September 24, 2020

In this work, we develop a finite differential hot-wire method to uncover the localized heat dissipation physics along microwires. The localized convection effect can be decoupled at the finite differential element with a spatial resolution of 10 microns. The heat convection coefficient is characterized from 314 W m^{-2} K to 1116 W m^{-2} K along different positions of microwires with different diameters, which decreases from wire ends to its middle point. The slope of temperature gradient at wire surface versus temperature is determined from 20150 m^{-1} to 8640 m^{-1}, which can be used to calculate the boundary layer thickness around microwires. © 2020 The Japan Society of Applied Physics

The increasing energy consumption and miniaturization of electronic devices create heat-dissipation challenges for thermal design, including the fields of micro-electro mechanical systems (MEMS), integrated circuits, microactuators and gas sensors.[1,2] Considerable efforts focus on the syntheses of electronic packaging materials[3] and thermal interface materials[4,5] with superior thermal conductivity, whereas the heat convection at micro/nanoscale is often out of emphasis. However, as the characteristic length of the sample is comparable or much smaller than the mean free path of gas molecules, heat convection is sensitive to frequent collisions of gas molecules, which could result in large proportion in heat dissipation.[6] To pave the way toward efficient thermal management, it is of great interest to characterize the convective heat loss in such a dimension.

The heat convection coefficient (h) evaluates the heat flux to temperature drop at the interface, which is used to quantify the microscopic energy coupling of the solid–gas interface.[7] At micro/nanoscale, the h has been demonstrated to be several orders of magnitude compared with that at the macroscale.[8] The decreasing size results in a weak buoyancy force of gas around the sample and thus significantly increases the convective heat loss.[9] It is speculated that the mechanism of heat convection at the microscale is different from that at the macroscale, that is, the heat convection mode becomes much close to heat conduction.[10] Besides, it is found that the contribution to the difference of micro-heat convection is the size of the heat source rather than the size of the sample.[11] However, the measured average h on the sample surface remains inconsistent with the value at different locations, which is called local h.[12] The localized energy coupling at solid–gas interface in a confined position could be modified by the localized conditions such as temperature, geometric parameters and surface treatment, which is especially vital for the sample at the micro/nanoscale.[13,14]

It is still challenging for estimating the local convective heat transfer mode at microscale due to the lack of effective available methods.[15] The confined size presents a problem for temperature detection, which is important for further localized heat convection analysis. The conventional methods of temperature measurements in contact ways such as resistance thermometer and thermocouples are no longer available due to the limited numbers of measurement points and the difficulty in monitoring point arrangement. For a non-contact manner, the micro-Raman spectroscopy method has been demonstrated as valid in characterizing the h.[16,17] A focused laser beam is employed to generate heating locally on the sample and the temperature response can be monitored spontaneously from the downshifts of the G-band frequency signal. In addition, when the temperature gradient of the thermal boundary layer (TBL) in the vicinity of the surface is determined, it is available to obtain the localized micro-heat transfer mode.[18]

In this work, we present a finite differential hot wire method for localized micro-heat transfer characterization. Thermal equilibrium for different discrete points related to the pixel of the infrared image is available for decoupling the localized heat convection, conduction and radiation effects. The localized heat transfer mode is determined at different temperatures and diameters. The thickness of the boundary layer around the microwire is determined from the slope of the temperature gradient at the wire surface versus temperature.

Figure 1(a) illustrates the schematic setup of the finite differential hot wire method. The microwire is suspended between two electrodes in atmospheric pressure with electrical heating. The joule heat is generated inside the wire and dissipates into the surrounding through conduction, convection and radiation heat transfer, which results in a difference of local temperature along the wire. One-dimensional thermal transport model is given as $\partial^2 T/\partial x^2 + \dot{Q}/k = 0$, where x is the distance away from the electrode, T is the wire temperature, k is the thermal conductivity and $\dot{Q}$ is local internal heat generation related to joule heating, heat convection and heat radiation. Similar to the numerical finite difference method,[19] the wire is separated into different discrete points, such as a total point number of $(n+1)$ in Fig. 1(b) with distance interval of Δx. In a small distance interval, the description of dT and dx could be replaced by ΔT and Δx. Therefore, the 1D energy conservation equation for a certain element i adjacent to element $(i-1)$ and $(i+1)$ can be calculated as

$$kA_c\left(\frac{T_{i-1}-T_i}{\Delta x}+\frac{T_{i+1}-T_i}{\Delta x}\right)+\dot{\Phi}+h_i P\Delta x(T_0-T_i)+\varepsilon\sigma P\Delta x(T_0^4-T_i^4)=0 \quad (1)$$

where A_c is the cross-section area and is described as $A_c = \pi D^2/4$, where D is the sample diameter. T_{i-1}, T_i and

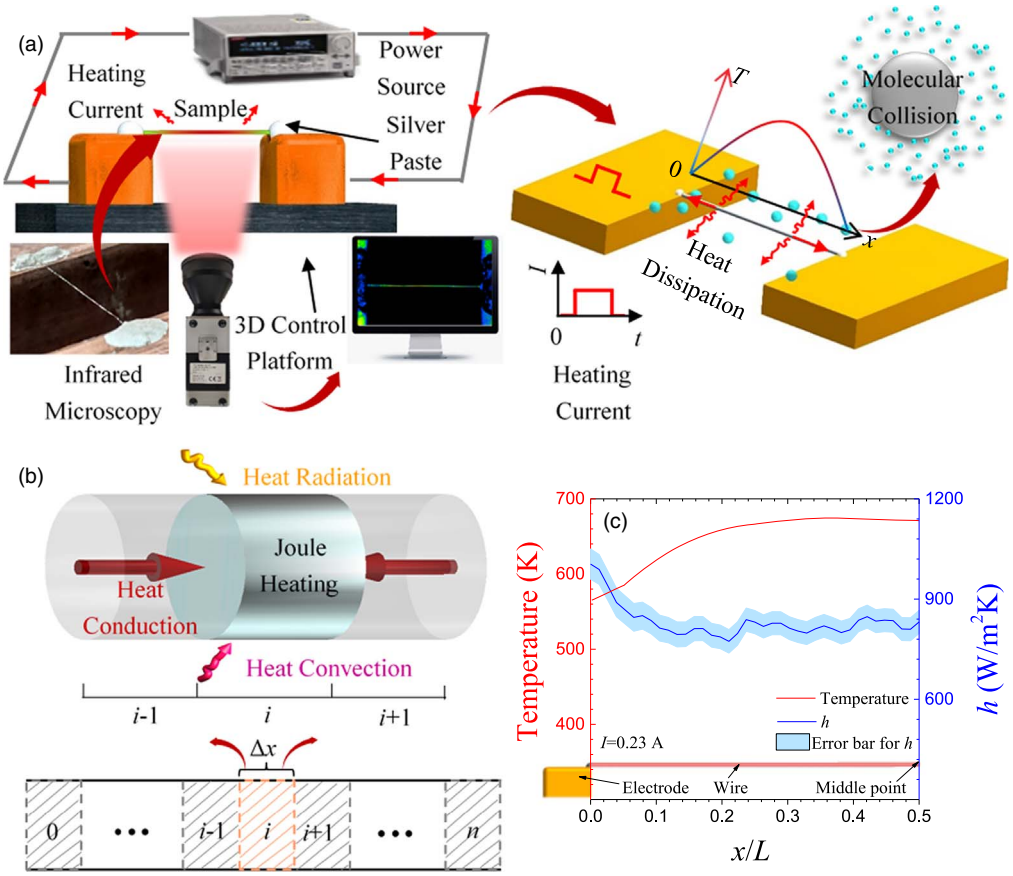

Fig. 1. (Color online) (a) Schematic setup of the finite differential hot wire method. (b) Energy conservation in discrete point. (c) Temperature profile (red line) and local h (blue line) as a function of dimensionless axial distance for microwire (25 μm) with a heating current of 0.23 A.

T_{i+1} is the temperature of element $(i-1)$, i and $(i+1)$, $\dot{\Phi}$ is the local joule heating calculated as $\dot{\Phi} = I^2\Delta R_i$, where I is the heating current, ΔR_i is the sample resistance, which is given as $\Delta R_i = \rho_e \Delta x/A_c$, where ρ_e is the sample electrical resistivity and is sensitive to the local temperature. h_i is the local heat convection coefficient, P is the cross-section perimeter and is determined as $P = \pi D$, T_0 is the room temperature, ε is the sample emissivity and σ is the Stefan–Boltzmann constant. When the local temperature is mapped along the wire, the local h at a discrete point is determined according to Eq. (1).

The platinum wires (thermal conductivity of 71.6 W mK^{-1} [20]) with a diameter varying from 20 to 40 μm are prepared in a length of 10 mm between two copper electrodes and immersed in air with a temperature of 298 K. The sample ends are attached with silver paste to achieve electrical connection with electrodes. The temperature profile along the wire is modified by applying heating currents from 95 to 320 mA, which is determined by infrared microscopy (InfraTech VarioCAM HD head 980) equipped with an optical lens (IR f/1.0 M = 1.0x LW JENOPTK) with a pixel resolution of 17 μm. The distance between infrared microscopy and sample can be adjusted by using a three-dimensional micro-control platform. The measured temperature at different locations along the platinum wire is sensitive to its emissivity. Specifically, as recommended by the manufacturer, we recalibrate the emissivity for our measurement target. The wire is uniformly heated more than 353 K on a hot plate. At the same time, the radiance energy emitted from the sample is recorded in each pixel of the detector, which is then compared to that of a blackbody at the same temperature in order to calculate the emissivity.[10] The emissivity of platinum wire is determined to be $0.09^{+0.003}_{-0.003}$, which is in good agreement with the literature.[21] In a further demonstration, the emissivity is found to be a stable value under different heating temperatures.

When a heating current of 0.23 A is applied to the microwire of diameter in 25 μm as shown in Fig. 1(c), the mapping temperature presents an increasing trend from the sample ends to the middle point in the range of 565–671 K, along with the local h decreases from 1004 to 810 W m^{-2} K. The uncertainty of h is sensitive to temperature, internal heat source and emissivity calculation. The decrease by 19.3% of h demonstrates that the local condition modifies the interaction between gas molecules and the hot surface, resulting in a difference in the local h in measurement. The h is two orders of magnitude larger than that at the macroscale,[22] which agrees well with the reported values[23] and our previous work.[24]

Figures 2(a)–2(d) show the temperature profiles along microwires in diameter of 20–40 μm under different heating currents, in which the temperature curves are painted with different colors according to the measured local h. Similar trends that the values of local h increase from the wire ends to the middle point are valid for all the samples. Since the energy coupling at the solid–gas interface is a diffusion thermal transport process through gas molecules, the development of the TBL modifies the local convective mode,

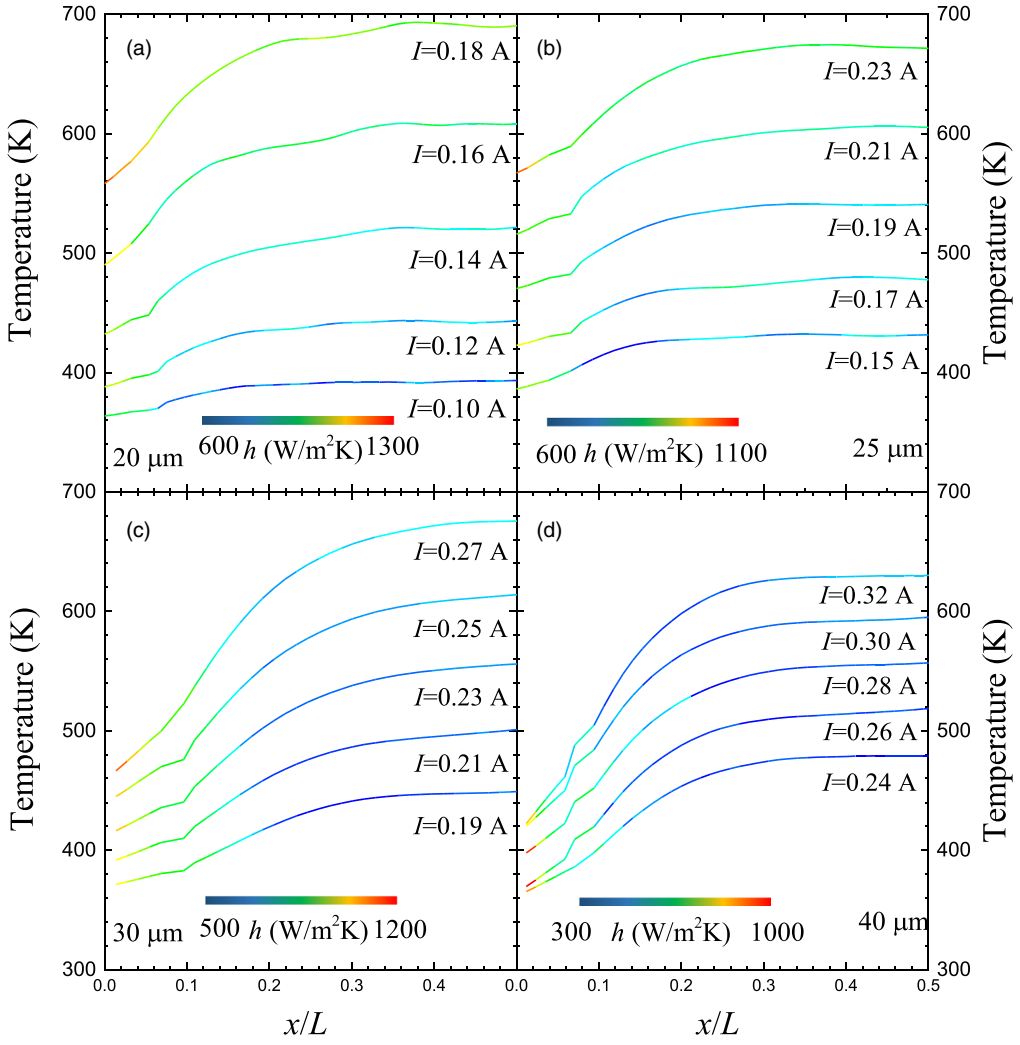

Fig. 2. (Color online) Temperature profiles from the sample end to the middle point on microwires in diameter of (a) 20 μm, (b) 25 μm, (c) 30 μm and (d) 40 μm with various heating currents.

which results in a variation of h at different locations.[25] Besides, it is found that the local h could evolve a decrease at the location with higher temperature along the microheater,[18] revealing a similar trend to our experiments.

Local h at the wire middle point is collected to uncover the mechanism of micro-heat transfer. The evolution trends of h with respect to temperature have been presented in Fig. 3. For a reference case of wire diameter in 20 μm, h evolves an increase from 642 $\mathrm{W\,m^{-2}\,K}$ to 1116 $\mathrm{W\,m^{-2}\,K}$ with increasing the temperature from 393 K to 733 K. The increase by 57% is ascribed to the modification of internal energy stochastic motions of gas molecules in TBL. Energy coupling between gas molecules and the solid surface consists of specular reflection (no energy exchange) and diffuse reflection (with energy exchange). In diffuse reflection, gas molecules reflected from a solid surface follow the Maxwell velocity distribution at the temperature of the solid surface. The collision frequency at higher temperature facilitates the diffuse reflection and results in an enhancement of h.

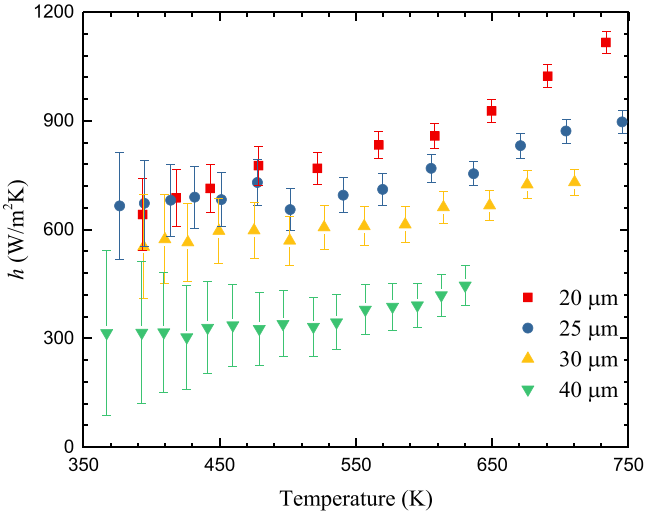

Fig. 3. (Color online) Local h at the middle point of wire under different temperatures.

Without flow separation around the microwire, the conductive heat loss from the microwire to adjacent air is given as $Q = -k_{\mathrm{air}}\,dT(r)/dr|_{\mathrm{surface}}$, where k_{air} is the thermal conductivity of air. Besides, the local h is defined as $h = Q/[T(r)|_{\mathrm{surface}} - T_0]$. When substituting the conductive heat loss, the correlation between the local h and

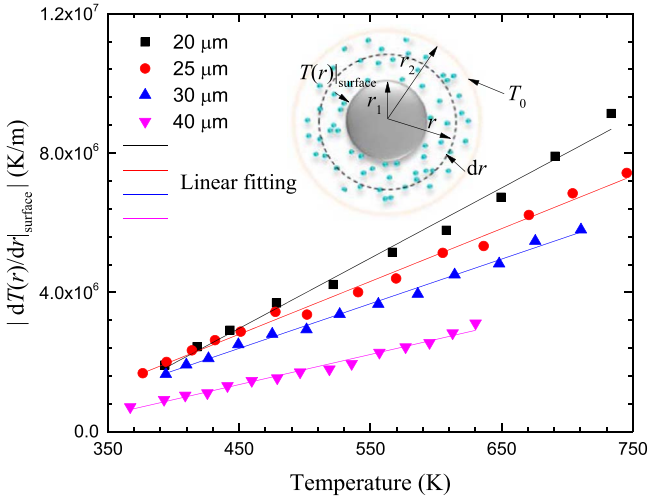

Fig. 4. (Color online) Temperature gradient adjacent to the solid surface with respect to wire temperature. The slope of the temperature gradient at the wire surface versus temperature from linear fitting is used to calculate the boundary layer thickness around microwires.

the TBL. Based on Eq. (2), we can calculate the derivation of the temperature gradient at wire surfaces versus temperature as

$$\frac{\partial[dT(r)/dr|_{\text{surface}}]}{\partial T(r)|_{\text{surface}}} = \frac{1}{r_1 \ln(r_2/r_1)}. \tag{3}$$

In Eq. (3), the values of r_2 can be determined from the slopes of the fitting line in Fig. 4, which are shown in Table I. It demonstrates that the boundary layer thickness around the microwire decreases as the wire diameter is decreased. Specifically, the (r_2-r_1) for microwire of diameter in 20 μm is determined as $1.42^{+0.29}_{-0.23} \times 10^{-3}$ m, which is close to the measured boundary layer thickness around a microheater.[18] The difference is attributed to the heater geometry and various measurement methods as selected.

Uncertainty of heat convection coefficient is sensitive to temperature, internal heat source and emissivity measurement according to Eq. (1). The absolute error of h_i is determined based on the differential formula as

$$\Delta h_i = \sqrt{\left(\frac{\partial h_i}{\partial T_{i-1}}\Delta T_{i-1}\right)^2 + \left(\frac{\partial h_i}{\partial T_i}\Delta T_i\right)^2 + \left(\frac{\partial h_i}{\partial T_{i+1}}\Delta T_{i+1}\right)^2 + \left(\frac{\partial h_i}{\partial T_0}\Delta T_0\right)^2 + \left(\frac{\partial h_i}{\partial \varepsilon}\Delta\varepsilon\right)^2 + \left(\frac{\partial h_i}{\partial \dot{\Phi}}\Delta\dot{\Phi}\right)^2} \tag{4}$$

$dT(r)/dr|_{\text{surface}}$ is established, which allows the calculation of $dT(r)/dr|_{\text{surface}}$ from the measured local h. The results of the temperature gradient adjacent to the solid surface have been shown in Fig. 4 under different temperatures. The absolute value of temperature gradient experiences an increase as the temperature is increased. At a certain wire temperature, this parameter is larger for a smaller wire diameter. The phenomenon is ascribed to the decreasing boundary layer thickness for the wire in a smaller diameter, resulting in a larger temperature gradient.[26]

Besides, it is found that the $|dT(r)/dr|_{\text{surface}}|$ presents a linear correlation with the wire temperature. The slopes of the fitting lines in Fig. 4 for microwires are determined by using the least square fitting method as presented in Table I, which decreases from 20150^{+725}_{-725} m^{-1} to 8640^{+300}_{-300} m^{-1}. The calculated coefficient of determination (R-square) is close to 1, revealing a remarkable linear correlation. As the conduction effect establishes the dominant mode in TBL,[27] the micro-heat transfer around the microwire could be simply considered as the heat conduction case similar to the concentric cylinder model as illustrated in the inset of Fig. 4. Therefore, we can obtain the temperature profile as[12]

$$T(r) = T(r)|_{\text{surface}} - [T(r)|_{\text{surface}} - T_0]\frac{\ln(r/r_1)}{\ln(r_2/r_1)} \tag{2}$$

where r is the distance away from the circle center, r_1 is the wire radius and r_2 is the distance from the air boundary to the circle center. Therefore, the term of (r_2-r_1) is the thickness of

where Δh_i, ΔT_{i-1}, ΔT_i, ΔT_{i+1}, ΔT_0, $\Delta\varepsilon$ and $\Delta\dot{\Phi}$ is the uncertainty of heat convection coefficient, temperature for element (i−1), temperature for element i, temperature for element (i+1), room temperature, emissivity and internal heat source, respectively. The temperature measured from infrared microscopy is 1 K in uncertainty (the real uncertainty would be much lower since we have performed the calibration). The uncertainty of room temperature measured by the thermocouple is 0.5 K, and the uncertainty of emissivity is determined to be 0.003. Since the internal heat source is calculated from the electrical resistivity and heating current, the uncertainty of internal heat source is given as $\Delta\dot{\Phi} = \sqrt{(2I\Delta x\rho_e\Delta I/A_c)^2 + (I^2\Delta x\Delta\rho_e/A_c)^2}$, where ΔI is the uncertainty for heating current with a relative uncertainty of 0.01, $\Delta\rho_e$ is the uncertainty for electrical resistivity (3.86×10^{-10} $\Omega \cdot$ m).

This work demonstrates the effectiveness of this finite differential hot-wire method by using the infrared technique. Because of the intrinsic limitations, the spatial resolution can be pushed down to 10 μm level. However, if the nanoscale thermal sensing technique is employed,[26] such as Raman thermometry,[28–30] fluorescence thermometry,[31–33] and so on, it is feasible to achieve a higher level of spatial resolution easily by switching the temperature mapping strategy from one-time imaging to the differential treatment of sample's spectroscopy signals.

In summary, a finite differential hot-wire method is developed to characterize the local-heat transfer behaviors along the microwire. The temperature profile at discrete

Table I. Calculated parameters for different microwires.

Diameter (μm)	20	25	30	40
$\frac{\partial[dT(r)/dr\|_{\text{surface}}]}{\partial T(r)\|_{\text{surface}}}$ (m^{-1})	20150^{+725}_{-725}	15146^{+390}_{-390}	12806^{+301}_{-301}	8640^{+300}_{-300}
Coefficient of determination (R-square)	0.9897	0.9921	0.9940	0.9846
(r_2-r_1) (m)	$1.42^{+0.29}_{-0.23} \times 10^{-3}$	$2.45^{+0.37}_{-0.31} \times 10^{-3}$	$2.72^{+0.37}_{-0.31} \times 10^{-3}$	$6.50^{+0.15}_{-0.12} \times 10^{-3}$

points from the infrared image is applied to determine the local h, which is demonstrated to be different at various locations. As the temperature is elevated, heat convection around microwire is enhanced and this correlation is even more obvious for a smaller diameter. The linear trends between the temperature gradient at the wire surface and wire temperature are uncovered to determine the boundary layer thickness, which decreases as the wire diameter is decreased.

Acknowledgments The support from the National Natural Science Foundations of China (Nos. 51576145, 52076156 and 51776142), Fundamental Research Funds for the Central Universities (No. 2042020kf0194), and the China Scholarship Council (No. 201906270144) are acknowledged.

ORCID iDs Jianshu Gao https://orcid.org/0000-0001-5442-0340

1) Y. Yue and X. Wang, Nano Rev. **3**, 11586 (2012).
2) J. Gao, H. Wu, A. Li, Y. Yue, D. Xie, and X. Zhang, ACS Appl. Nano Mater. **2**, 6828 (2019).
3) C. Chen, Y. Xue, X. Li, Y. Wen, J. Liu, Z. Xue, D. Shi, X. Zhou, X. Xie, and Y. Mai, Compos. Part A-appl. S. **118**, 67 (2019).
4) W. Dai et al., ACS Nano **13**, 1547 (2019).
5) J. Gao, C. Meng, D. Xie, C. Liu, H. Bao, B. Yang, M. Li, and Y. Yue, Appl. Therm. Eng. **150**, 1252 (2019).
6) J. Zhang, E. Strelcov, and A. Kolmakov, Nanotechnology **24**, 444009 (2013).
7) H. Wahyudi, K. Chu, and A. Yu, Int. J. Heat Mass Tran. **97**, 521 (2016).
8) A. Giri and P. E. Hopkins, J. Chem. Phys. **144**, 084705 (2016).
9) Z. Huang, J. Wang, S. Bai, J. Guan, F. Zhang, and Z. Tang, IEEE T. Ind. Electron **64**, 7387 (2017).
10) P. Liu, Z. Fan, A. Mikhalchan, T. Tran, D. Jewell, H. Duong, and A. Marconnet, ACS Appl. Mater. Inter. **8**, 17461 (2016).
11) R. Pulavarthy, M. Alam, and M. Haque, Int. Commun. Heat Mass **52**, 56 (2014).
12) T. Bergman, F. Incropera, D. DeWitt, and A. Lavine, *Fundamentals of Heat and Mass Transfer* (Wiley, New York, 2011).
13) S. Wong and W. Lee, Int. J. Therm. Sci. **138**, 116 (2019).
14) S. Haghighi, H. Goshayeshi, and M. Safaei, Int. J. Heat Mass Tran. **125**, 640 (2018).
15) D. Han, G. Li, S. Zhou, Z. Wang, F. Yang, and S. Xu, RSC Adv. **7**, 9100 (2017).
16) H. Wang, J. Liu, Z. Guo, X. Zhang, R. Zhang, F. Wei, and T. Li, Nanosc. Microsc. Therm. **17**, 349 (2013).
17) M. Li, C. Li, J. Wang, X. Xiao, and Y. Yue, Appl. Phys. Lett. **106**, 253108 (2015).
18) M. Alam, A. Raghu, M. Haque, C. Muratore, and A. Voevodin, Int. J. Therm. Sci. **73**, 1 (2013).
19) Y. Gu, Q. Hua, C. Zhang, and X. He, Appl. Math. Model. **71**, 316 (2019).
20) S. Azarfar, S. Movahedirad, A. Sarbanha, R. Norouzbeigi, and B. Beigzadeh, Appl. Therm. Eng. **105**, 142 (2016).
21) C. Xing, C. Jensen, T. Munro, B. White, H. Ban, and M. Chirtoc, Appl. Therm. Eng. **73**, 317 (2014).
22) Ş. Atayılmaz, Int. J. Therm. Sci. **50**, 1472 (2011).
23) Z. Wang and D. Tang, Int. J. Therm. Sci. **64**, 145 (2013).
24) J. Gao, D. Xie, Y. Xiong, and Y. Yue, Appl. Phys. Express **11**, 066601 (2018).
25) V. Kumar, M. Kumar, and C. Shakher, Appl. Optics **53**, G74 (2014).
26) N. Guan, Z. Liu, C. Zhang, and G. Jiang, Heat Mass Transfer **50**, 275 (2014).
27) T. Zhu and W. Ye, Numer. Heat Tr. B-fund. **57**, 203 (2010).
28) Y. Yue, J. Zhang, and X. Wang, Small **7**, 3324 (2011).
29) J. Liu, H. Wang, Y. Hu, W. Ma, and X. Zhang, Rev. Sci. Instrum. **86**, 014901 (2015).
30) R. Wang, H. Zobeiri, Y. Xie, X. Wang, X. Zhang, and Y. Yue, Adv. Sci. **7**, 2000097 (2020).
31) J. Gu, J. She, and Y. Yue, ES Energy Environ (2020).
32) R. Wang, S. Xu, Y. Yue, and X. Wang, Int. J. Extreme Manuf **2**, 032004 (2020).
33) C. Li and Y. Yue, Nanotechnology **25**, 435703 (2015).